Journal of Applied Electrochemistry **34**: 151–158, 2004.

Dissolution from electrodeposited copper–cobalt–copper sandwiches

S.M.S.I. DULAL, E.A. CHARLES and S. ROY*
Corrosion Centre, School of Chemical Engineering and Advanced Materials, Merz Court, University of Newcastle, Newcastle-upon-Tyne, NE1 7RU, UK
*(*author for correspondence, fax: +44-191-222-5292; e-mail: s.roy@ncl.ac.uk)*

Received 19 August 2002; accepted in revised form 3 September 2003

Key words: Cu/Co multilayers, cyclic voltammetry, electrodeposition, electrodissolution, rotating ring disc electrode

Abstract

The electrochemical behaviour of electrodeposited Co–Cu/Cu multilayers from citrate electrolytes was investigated using cyclic voltammetry and stripping techniques at a rotating ring disc electrode. Copper and cobalt–copper alloy sandwiches were deposited from an electrolyte containing 0.0125 M $CuSO_4$, 0.250 M $CoSO_4$ and 0.265 M trisodium citrate at two different pHs, 1.7 and 6.0. The Cu/Co–Cu/Cu sandwich is representative of a single layer in a Co–Cu/Cu multilayer deposit, which is known to exhibit unusual physical and magnetic properties. Results from cyclic voltammetry and detection of dissolving species at the ring showed that cobalt is stripped from a Cu/Co–Cu/Cu sandwich even when a copper layer as thick as 600 nm covers the Co–Cu alloy. Scanning electron microscopy showed that cobalt can dissolve from the deposit easily because the copper layer covering the Co–Cu alloy is porous. A separate series of experiments with Cu/Co–Ni–Cu/Cu sandwich showed that cobalt does not dissolve from these deposits because the addition of nickel stabilises cobalt in the Co–Ni–Cu alloy.

1. Introduction

Thin films of metal or alloy multilayers of copper and nickel, copper and cobalt, or copper and nickel–iron alloy exhibit unusual physical and mechanical properties, which has engendered a lot of interest in the last two decades. Until the mid-nineties, most investigations concentrated their efforts on the search for the optimal combination of metals (or alloys) [1, 2], substrates [2, 3], layer thicknesses [4, 5], crystal orientation [1–4] etc., to improve deposit properties. Although many kinds of metal multilayer have been fabricated by electrodeposition, relatively less attention has been paid to the determination of the effect of electrochemical processes influencing deposit composition, bi-layer thicknesses and hence, their properties.

Two different electrochemical techniques have been proposed to deposit metal multilayers. The first is electrodeposition from a single electrolyte where small quantities of the more noble metal and large quantities of the less noble metal are present. Alternate layers of the two metals are obtained by depositing the noble component at the diffusion limiting current, and then plating the less noble component under kinetic control. The second technique involves the use of two separate electrolytes and the substrate is transferred from one to the other, where each metal is plated. The single bath method has gained more popularity because it uses simpler apparatus, lowers the possibility of contamination or oxidation and is more efficient for plating layers of nano-metric thicknesses, where enhanced physical properties are often observed.

One major problem of multilayer electrodeposition process is that the less noble metal can dissolve during the deposition of the noble component. The problem was first reported by Despić and Jović [6] in the Pb/Cu system. They found that during the current off period, copper underwent a displacement reaction with lead and lead dissolution occurred. Tench and White proposed a method for depositing metal multilayers of Ag/Cu using pulse current [7]. They proposed that the less noble layer could be plated by applying a high pulse current, then the current should be turned off. They found that during this time the less noble component is displaced by the more noble one, forming a layer rich in that component and also that this process continued through relatively thick Ag layers.

A more thorough and quantitative description of displacement reaction during pulse plating was provided by Roy et al. [8] for the deposition of Ni–Cu alloys from a citrate electrolyte. They showed that the displacement reaction occurred because the metal system reached an open circuit potential where galvanic corrosion occurred. Later Roy and Landolt [9] showed that nickel dissolution was stifled quickly by the formation of a 1.5–10 nm Cu-rich layer formed due to the displacement

reaction. Bradley et al. showed that this description was also valid for Cu–Ni alloys plated from sulphamate electrolytes [10], and that 5–10 monolayers of plated copper stifled the displacement reaction [11]. A later study by Bradley and Landolt, where copper and cobalt alloys were electrodeposited from a citrate electrolyte, however, showed that the dissolution of cobalt continued for much longer time periods compared to the copper–nickel system [12]. *Ex situ* SEM examination [12] revealed that microstructure of the cobalt was columnar or dendritic, which allowed the cobalt to dissolve from the deposit. Kelly et al. showed that cobalt dissolution can continue indefinitely if the cobalt is sufficiently rough [13] and that two-dimensional Co-rich and Cu-rich structures may be formed during the pulsed current plating of Cu–Co alloys [14], which leads to cobalt dissolution. Shima et al. [15] showed that a certain degree of phase separation and segregation occurs in Co/Cu laminates, which can lead to cobalt dissolution from beneath a copper layer.

The above mentioned pulse current studies raise new questions regarding Co/Cu multilayers deposited by the single bath technique. Since this technique is an extrapolation of pulse plating (instead of switching off the current, a low current is applied during the off time), it is important to understand if cobalt can dissolve from a deposit when copper is being deposited. It has been noted that magnetoresistance of Co–Ni/Cu multilayers is dependent on solution pH [16]. Since copper and cobalt speciation in solution change with electrolyte pH (and hence affect adsorption as well as discharge processes at the electrode) [17], it is important to understand if cobalt dissolution is pH dependent. This also bears support from studies that show that electrodeposited cobalt has fcc and hcp structures when deposited from $CoSO_4$ solutions with pH equal to 2 or 6, respectively [18].

The present work was undertaken to determine if cobalt can dissolve from 'beneath' a copper layer when plated from a citrate electrolyte. This electrolyte was chosen because it has been used by a number of researchers to plate metal multilayers. Cyclic voltammetry was used to identify the deposition and dissolution potential ranges for copper and cobalt in a $CuSO_4$/$CoSO_4$/trisodium citrate (Na_3Cit) solution. A copper–cobalt–copper sandwich, which is representative of a single composition modulation in a Co/Cu multilayer deposit, was deposited at a rotating ring disc electrode (RRDE). The sandwich was plated at the disc electrode by changing the disc potential with time, similar to the potential changes in cyclic voltammetry. At the same time, species dissolving from the disc were monitored at the ring electrode.

2. Experimental

Electrodeposition was carried out from electrolytes containing either 0.0125 M Cu(II) or 0.25 M Co(II) or both. The electrolytes were prepared by dissolving $CuSO_4 \cdot 5H_2O$ and $CoSO_4 \cdot 7H_2O$ in ultra pure water. An appropriate amount of trisodium citrate (Na_3Cit), a complexing agent, was added to maintain its concentration at 0.265 M in all solutions. The pH of electrolytes was adjusted to either 1.7 or 6.0 by adding dilute H_2SO_4 or NaOH. All chemicals were of analytical grade. The electrolytes were not de-aerated prior to experiments. The oxygen discharge current during the experiments was 10 A m^{-2}, which did not influence the interpretation of any of our results.

A RRDE apparatus with a gold working electrode was used in the experiments. The disc diameter was 7 mm and the inner and outer diameters of the ring were 7.5 and 8 mm, respectively. The RRDE was mechanically polished with grade 4000 silicon carbide paper and rinsed with acetone and air dried. The rotating shaft was placed in a Perspex cylindrical tank and rotated at 1200 rpm in all experiments. A platinum coated titanium mesh was used as a counter electrode. All potentials were measured against a standard mercury sulphate electrode (SME) placed approximately 1 cm away from the RRDE. Cyclic voltammetry and copper–cobalt–copper sandwich deposition with simultaneous detection of dissolving species at the ring was performed using a Model 366A bi-potentiostat. In all experiments, potential scans commenced at 0.00 V vs the SME. The potential was swept at a rate of either 0.010 or 0.012 V s^{-1}.

Prior to deposition experiments, the collection efficiency of the ring electrode of the RRDE was determined using the redox system

$$Fe(CN)_6^{-3} + e^- \longleftrightarrow Fe(CN)_6^{-4} \quad (1)$$

A solution of 0.005 M $Fe(CN)_6^{-4}$ and 0.5 M KCl was used in these experiments. The disc potential was held at 0.70 V vs a saturated calomel electrode (SCE), where ferrocyanide was oxidised to ferricyanide. The ring potential was held at −0.30 V vs SCE where the reverse reaction occurred. Currents at ring and disc electrodes were noted at different rotation speeds between 400 and 1600 rpm. It was found that the average collection efficiency was 0.188 and the spread was within ±5% of this value. This is in good agreement with the theoretical current efficiency of 0.190, as obtained from the radii of the disc and ring [19, 20].

3. Results and discussion

3.1. *Cyclic voltammetry of Cu(II) and Co(II) in citrate electrolytes*

Figure 1 illustrates the proportion of copper and cobalt species in a solution containing 0.0125 M $CuSO_4$, 0.250 M $CoSO_4$ and 0.265 M Na_3Cit between pH = 0 and pH = 8. The speciation calculations were performed using MINEQL+ [21] and the stability con-

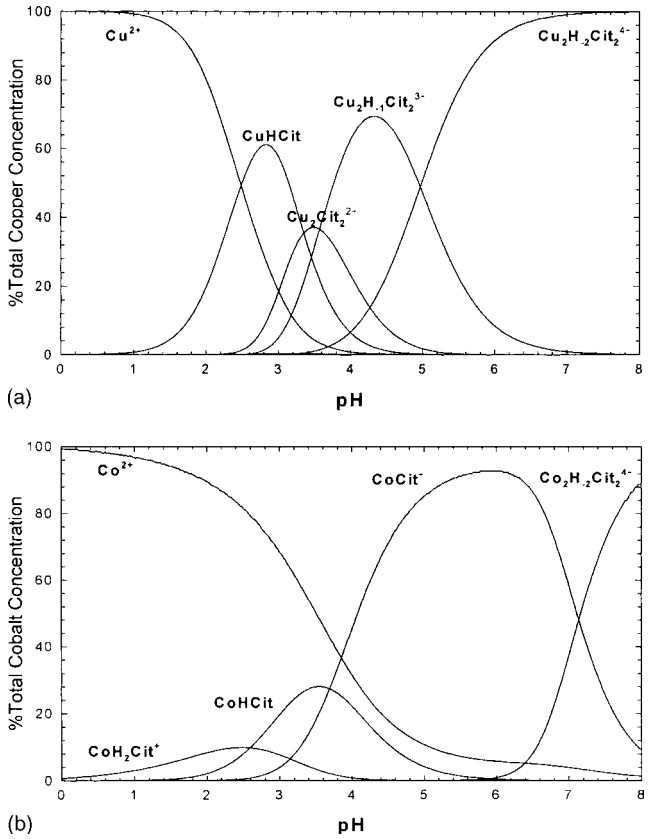

Fig. 1. Speciation of (a) copper and (b) cobalt in a solution containing 0.0125 M $CuSO_4$, 0.25 M $CoSO_4$ and 0.265 M Na_3Cit.

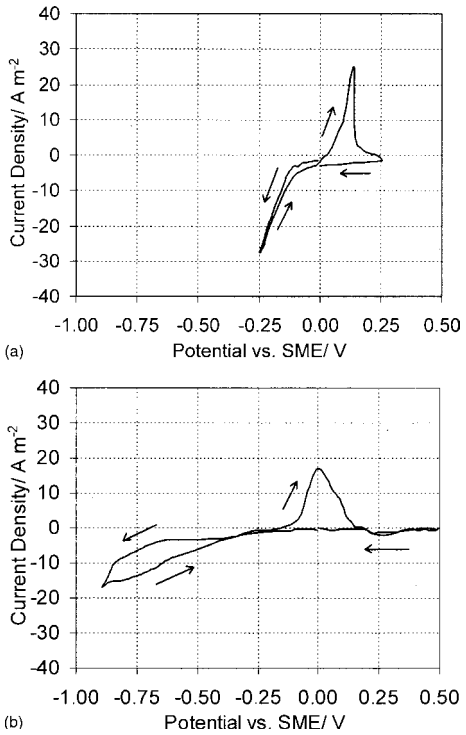

Fig. 2. Cyclic voltammogram for an electrolyte containing 0.0125 M $CuSO_4$ and 0.265 M Na_3Cit. (a) pH = 1.7 and (b) pH = 6.0. Disc rotation speed is 1200 rpm. Potential sweep rate (a) 0.010 V s^{-1} and (b) 0.012 V s^{-1}.

stants from [17]. Notably, Co(II) can form $CoCit^-$ ($\log \beta = 5.0$), CoHCit ($\log \beta = 8.7$) and CoH_2Cit^+ ($\log \beta = 11.28$) with citrate ions. A detailed description for the method of calculation is provided in [22]. Notably, Cu(II) and Co(II) are the dominant species at pH = 1.7. At a pH = 6.0, the dominant species for copper is $Cu_2H_{-1}Cit_2^{3-}$ and cobalt is $CoCit^-$ (here H_{-1} refers to the removal of the fourth proton of the citrate ion; this proton is extracted from the hydroxyl group). This speciation diagram indicates that copper and cobalt are discharged from different species at the two different pHs, and may have different electrochemical behaviours.

Cyclic voltammograms of copper reduction and oxidation in a citrate electrolyte of pH 1.7 and 6.0 are shown in Figure 2. The electrolyte used in this experiment did not contain any Co(II) ions and is therefore a 'copper-only' electrolyte. Several scans were carried out with different limits for the potential scan. The scan limits were set at −0.10 and 0.10 V in the first scan and were then increased by ±0.05 V in each direction in subsequent scans. Figure 2a shows the potential scan between −0.25 and 0.25 V. Although a small deposition current is observed at −0.10 V, this current is mainly due to oxygen reduction. Integration of the anodic and cathodic charges reveals that no significant deposition occurs until the electrode potential reaches −0.20 V. As the potential is reversed and swept to more positive values, an oxidation current is observed beyond 0.10 V. The dissolution current falls as most of the copper is dissolved.

Figure 2b shows a typical cyclic voltammogram for a copper only electrolyte at pH 6.0. The figure shows that a reduction reaction occurs at potentials more negative than −0.40 V; however, no oxidation peak was observed when the scan was reversed at −0.80 V. The reduction current observed between −0.40 and −0.80 V was therefore attributed to oxygen reduction. As shown in the figure, a peak for copper oxidation is observed when the cathodic scan limit is increased to −0.90 V. The current for copper reduction remains small, which is consistent with copper reducing from a complex species [17, 18]. As the potential is swept in the opposite direction, the discharge current is found to be higher. This hysteresis indicates that copper nucleates more easily on copper than on gold (since, on the outward scan, copper nucleates on the gold electrode, and in the backward scan, copper plates on a copper covered electrode). As the potential is scanned in the positive direction, copper dissolution commences at −0.10 V. This shows that in the pH 6.0 solution, copper reduction and oxidation occur at potentials less negative than those in the pH 1.7 solution, as can be expected when copper is complexed. A comparison of the charge in the cathodic (starting at −0.80 V) and anodic cycles, and correcting for oxygen discharge, showed that copper plated at the electrode was balanced by copper dissolution.

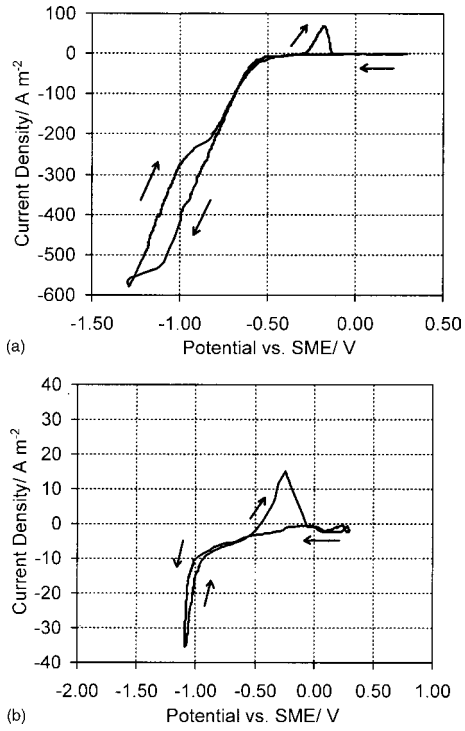

Fig. 3. Cyclic voltammogram for a 0.25 M $CoSO_4 \cdot 5H_2O$ and 0.265 M Na_3Cit electrolyte. Disc speed is 1200 rpm; (a) pH = 1.7 and sweep rate 0.010 V s^{-1}; (b) pH = 6.0 and sweep rate 0.012 V s^{-1}.

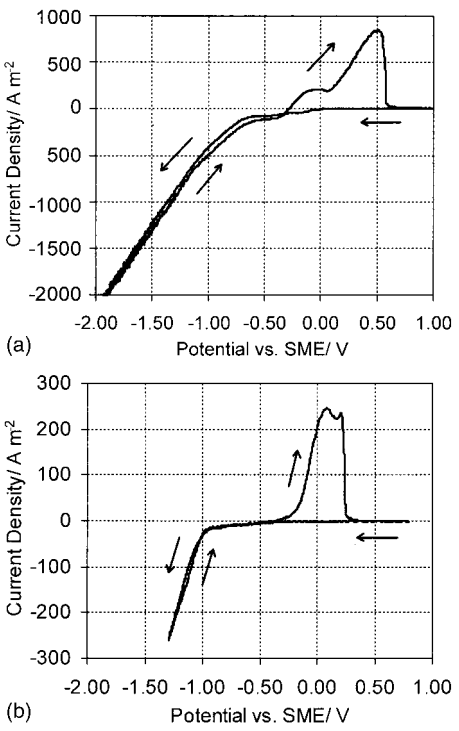

Fig. 4. Cyclic voltammogram for an electrolyte containing 0.0125 M $CuSO_4$, 0.25 M $CoSO_4$ and 0.265 M Na_3Cit. Rotation speed is 1200 rpm. Potentials sweep rate is 0.010 s^{-1}, (a) pH 1.7 and (b) pH 6.

Figure 3a shows a voltammogram of cobalt reduction and oxidation in a citrate electrolyte of pH 1.7, i.e. for a cobalt-only solution. Since hydrogen evolution commenced before cobalt reduction, a series of voltammetry experiments with different potential scan limits were performed to determine the reversible potential for cobalt. Although a reduction current was observed at −0.60 V, the lack of any oxidation peak in the anodic sweep showed that Co reduction did not occur up to −1.1 V for a Co-only electrolyte at pH 1.7. Therefore, the reduction current between −0.60 and −1.1 V is attributed to oxygen and proton reduction at the electrode. When the scan is reversed, cobalt dissolution commenced at −0.25 V and continued until all the cobalt was dissolved from the electrode. A comparison of the deposition charge for the co-discharge of cobalt and hydrogen (between −1.1 and −1.5 V), and the dissolution charge of cobalt, as shown in Figure 3a, showed that the cobalt partial current contributed to only ca. 3% of the overall charge passed.

Figure 3b shows cobalt oxidation and reduction from a pH 6.0 electrolyte. A reduction current was observed at −0.50 V, but this current was due to oxygen or proton reduction (no oxidation peak). The current remained low until −1.0 V and increased rapidly after that, and as can be inferred from the observed oxidation peak, Co(II) reduction takes place at potentials more negative than −1.0 V. This value is comparable to that for the pH 1.7. An integration of charges for cobalt deposited and dissolved shows that all the metal plated in the cathodic sweep is dissolved during the anodic sweep.

Figure 4 shows cyclic voltammograms of electrochemical oxidation and reduction for copper and cobalt from a solution containing both metal ions and sodium citrate. Copper discharge began at −0.20 V, as was observed in the copper-only solution. However, it was found that Co(II) did not reduce at −1.0 V, as was found in the cobalt-only solution, but did reduce at −1.5 V (from a series of potential scans). The more negative potential necessary for cobalt discharge in the mixed metal system is attributed to the higher energy required by cobalt to nucleate on copper; in the cobalt-only experiment, Co(II) was nucleating on gold. When the scan was reversed, an anodic current was observed at −0.30 V. The dissolution current exhibits an indistinct peak between −0.30 and 0.10 V followed by a more distinct peak at more positive potentials. The first oxidation peak is observed at a potential close to the cobalt dissolution peak (cf. Figure 3a). The two peaks may be due to the dissolution of cobalt, copper, or copper–cobalt alloy.

Figure 4b shows a voltammogram for the same solution for which the pH had been adjusted to 6.0. In this case, copper deposition commenced at a potential slightly more negative than −0.80 V, as was found in the copper-only experiments. As observed previously, the copper deposition current remained low. Co(II) discharge is observed more negative than −1.0 V, as was observed in the cobalt-only solution at pH 6.0. As the potential was scanned in the positive direction, a dissolution current appeared at potentials positive of −0.30 V, which lies between the copper and

cobalt oxidation potentials determined from the separate metal solutions (Figures 2b and 3b). In addition, there is a semblance of a split peak, although it is not as clear as that observed in Figure 4a. This suggests that the dissolution of plated metals occurs in more than one step, as was found for the deposit plated at pH 1.7.

3.2. *Cu/Co/Cu deposition experiments*

The voltammetric results suggest that graduated metallic layers will be obtained from the system studied. For example, Figure 4a indicates that a copper layer would be obtained between −0.10 and −1.5 V, because Co(II) does not co-discharge at these potentials. At more negative potentials, however, both copper and cobalt will co-discharge (between −1.5 and −2.0 V), and will continue to do so during the reverse scan. Thus, scanning the potential over a broad range will form a Co–Cu alloy with graduated composition; going from Cu-rich to Co-rich and then back again to Cu-rich. Below −1.50 V, again, only copper plates and a copper layer will cover the Cu–Co alloy. Thus, a sandwich of Cu/Co–Cu/Cu was formed during the potentiostatic cycling experiment.

A second point is that anodic dissolution commences in Figure 4a and b at −0.30 and −0.40 V, respectively, where copper can not oxidise (cf. Figure 2a and b). However, as explained in the previous paragraph, at the beginning of dissolution, there is only pure copper in contact with the electrolyte. This indicates that either a copper–cobalt phase is formed at the surface (by migration of cobalt to the surface) or that the copper layer on top of the cobalt is relatively rough and porous. There is also the possibility of the formation of Cu-rich and Co-rich phases as described by Kelley et al. [14], and that the two peaks correspond to dissolution of the two phases.

In order to separate the peaks observed in Figure 4, a set of experiments was carried out where Cu/Co–Cu/Cu sandwiches were formed by potential cycling at 0.010 V s^{-1}. The sweep rate was decreased to 0.002 V s^{-1} as soon as the potential reached the value at which anodic currents had been observed, i.e. −0.30 V at pH 1.7 and −0.40 V at 6.0. As shown in Figure 5a, it was found that anodic current increased at potentials more positive than −0.30 V, reached a peak, and then decreased to zero at −0.05 V. As the electrode potential was increased further, as second peak appeared between −0.05 and 0.25 V. A similar result was obtained with the pH 6.0 electrolyte, which is shown in Figure 5b. The two anodic peaks are much smaller that those observed in Figure 4; this is due to the slower potential sweep rate. The plating and stripping charges in Figures 4 and 5 are comparable.

The data in Figure 5 shows clearly that the mixed metal deposits dissolved as two separate phases. Interestingly, the first dissolution peak is observed at potentials between −0.30 and −0.05 V in Figure 5a,

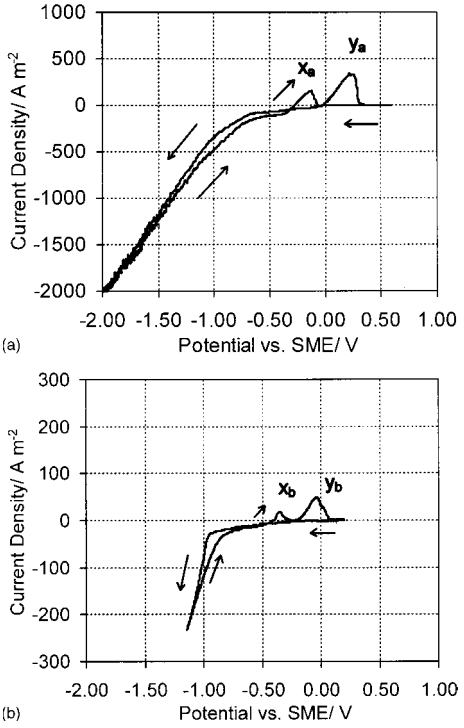

Fig. 5. Cyclic voltammogram for an electrolyte containing 0.0125 M $CuSO_4$, 0.25 M $CoSO_4$ and 0.265 M Na_3Cit. Disk rotation speed is 1200 rpm. (a) pH 1.7 with sweep rates of 0.010 –0.002 V s^{-1}; (b) pH 6 with sweep rates of 0.012 and 0.002 V s^{-1}.

and −0.40 and −0.20 V in Figure 5b. This peak lies in the range where cobalt or a cobalt-rich phase should dissolve (cf. Figure 3). The peak at more positive potentials is observed where copper or a copper-rich phase is expected to dissolve. Since the cobalt-rich phase is buried beneath the copper-rich phase, the copper-rich phase must be porous or unstable, or possibly, both.

In order to identify the metallic phases associated with the various layers within the deposit, the dissolving species were detected at a ring electrode as the potential of the disc electrode was cycled. The scan rate was comparable to that used for Figure 4a. In this case, a Cu/Co–Cu/Cu sandwich was deposited at the disc surface and was stripped during the anodic potential scan; the dissolving species was monitored at the ring electrode. Figure 6a shows the ring current at a disc potential at −0.60 V, at which only Cu(II) was detected during the deposition and dissolution of a Cu/Cu–Co/Cu sandwich. The experimental conditions were identical to those used to collect data at the disc in Figure 4a. The potential at the disc electrode as a function of time is displayed on the *x*-axis at the top.

As can be seen in Figure 6, at the start of the cathodic scan, the ring current density is −200 A m^{-2}, which is apparently due to the discharge of oxygen and Cu(II) reduction from the bulk solution. As the disc potential is scanned to more negative values, there is a gradual decrease in the ring reduction current to a low value. This is due to the shielding effect of the disc; i.e. all

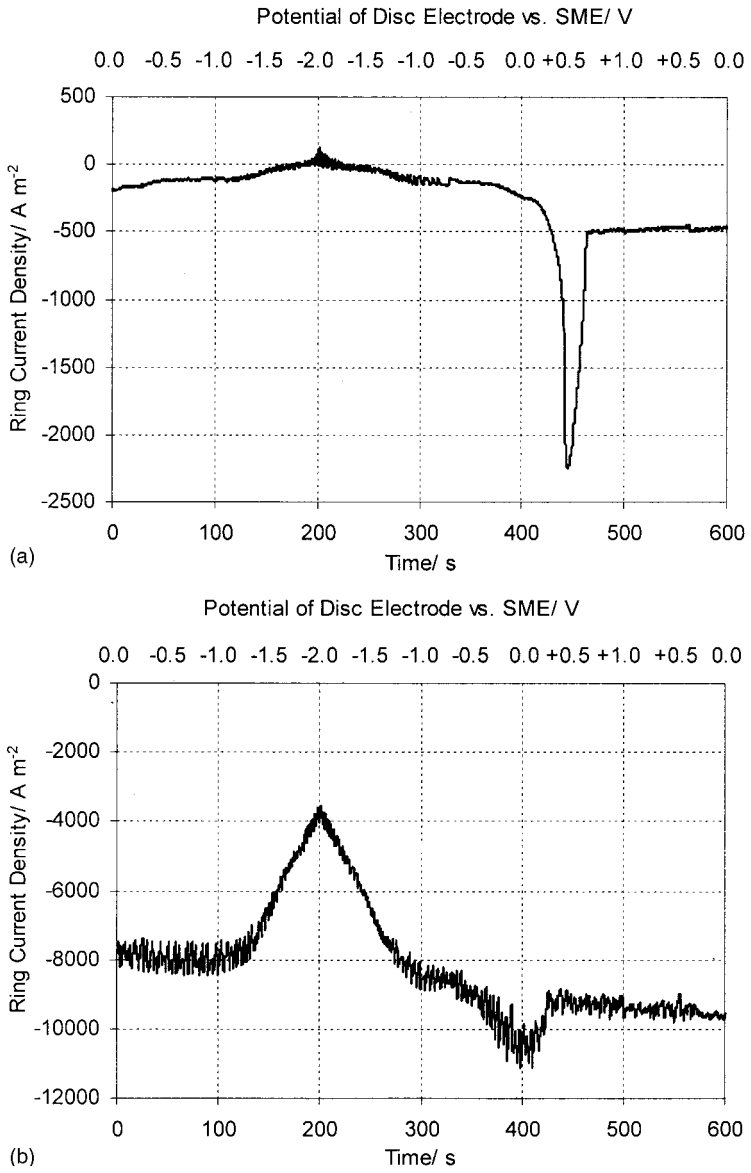

Fig. 6. Current vs time data at the ring electrode when the disc potential was swept under the same conditions as in Figure 4a. (a) ring-electrode held at −0.60 V where only Cu(II) is expected to reduce, and (b) ring electrode held at −1.60 V where Co(II) is expected to discharge.

Cu(II) ions and oxygen are consumed at the disc (copper is plating at its limiting current), and almost none is reduced at the ring electrode.

As the disc potential is swept to more positive values, the current increases to the original value corresponding to reduction of species from the bulk electrolyte. At −0.10 V there is a small rise in the reduction current. A subsequent sharp rise in reduction current is observed when the disc potential reaches 0.20 V, after which the current drops to a value which is higher than that observed for bulk Cu(II) deposition previously.

Detection of Co(II) was only partially successful since, as shown in Figure 6b, the current for potential needed to detect Co(II) was noisy due to simultaneous hydrogen evolution. However, an increase in ring current is observed when the disc potential reached −0.50 V, the potential at which only Co(II) can be reduced. There is a clear peak around 0.00 V, due to the additional current contributed by Cu(II) reduction, as the copper layer on the disc begins to dissolve.

As seen by comparison of Figures 5a and 6a, the first peak in Figure 6a occurred before the disc potential reached −0.10 V. Therefore, it can be concluded that copper does not dissolve when the first anodic dissolution peaks, marked as x_a and x_b, are observed. Copper reduction at the ring, in fact, is observed when the second dissolution peaks, i.e. y_a and y_b, are observed at the disc. In addition, the estimated charge for copper reduction during the formation of a multilayer at pH 1.7 is 1.25 C, and that obtained by integrating the charge under the second peak is 1.22 C. The charge integrated at the ring, with a correction for current efficiency, is 1.26 C. The ring reduction current data, therefore, clearly point to cobalt dissolution from the deposit occurring when the first peak (x_a, x_b) is observed. The thickness of copper formed on top of the Cu–Co alloy is

estimated to be 600 nm. This indicates that the cobalt in this layer can migrate or is exposed through the copper over-layer to the surface.

3.3. *Implications for Co/Cu and Co–Ni/Cu metal multilayers*

As discussed in the introduction, nickel dissolution during the deposition of copper layer is stifled very quickly [9, 11], possibly due to the passivation of nickel [23]. Therefore, it is worthwhile to examine if the presence of nickel in the Co/Cu system can affect the dissolution behaviour. Figure 7 shows a cyclic voltammogram where 0.7 M Ni(II) was present with copper and cobalt in a citrate electrolyte of pH 6.0. The electrolyte composition was similar to that generally used to fabricate Ni–Co/Cu multilayers [23, 24]. The potential was swept up to −1.50 V at 0.012 V s^{-1}. It was found that the dissolution of the deposit commenced around 0.0 V during the reverse scan.

As found previously, anodic dissolution of copper begins around 0.0 V for a solution pH of 6.0, which corresponds to copper oxidation. Hence the first peak in the anodic cycle is due to dissolution of the top layer of copper covering the Co–Ni–Cu layer. The alloy starts to dissolve thereafter. This is clearly different from the copper–cobalt system. The change in electrochemical behaviour could be due to the formation of a phase which either stabilises cobalt in the alloy, or passivation of the alloy. It is well known that cobalt is immiscible in copper, and our cyclic voltammetry experiments show that cobalt does not nucleate well on copper; this may mean that copper and cobalt exist as nano-particulates in the Cu–Co layer instead of a homogeneous alloy, which allows dissolution to occur. The Ni–Cu system, on the other hand, is completely miscible, and therefore produces a uniform alloy layer.

In order to determine if there is any significant difference in the structure of Cu/Co–Cu/Cu and Cu/Co–Ni–Cu/Cu sandwiches, scanning electron microscopy (SEM) was carried out. These experiments were performed in a flow cell described elsewhere [23–25] because RRDE or RDE electrodes were inappropriate for SEM examination. In these experiments, sandwiches were deposited on circular glass sputtered with Cr and Au. The electrolyte composition and pH were the same as that used in the RRDE experiments. In this experiment, the potential was swept negative to −1.50 V at a rate of 0.012 V s^{-1}. The scan was stopped when the potential reached −0.20 V during the anodic scan, and the disc was held at this potential for 3 min; thereafter the potentiostat was switched off and the glass disc was removed.

Figure 8 shows the SEM images of Cu/Co–Cu/Co and Cu/Co–Cu–Ni/Cu sandwiches obtained by this method. As can be seen the former is porous with 50–200 nm pores. The latter is granular but there are no pores. This shows that the copper layer covering the Cu–Co and Cu–Ni–Co alloys is also different; possibly the nucleation of copper on cobalt is less uniform which leaves pores through which the Cu–Co layer can be accessed by the electrolyte. As far as the fabrication of metal multilayers is concerned, our results show that

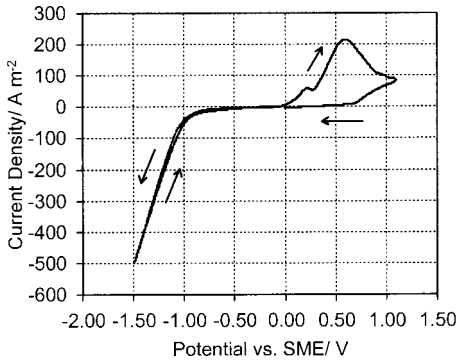

Fig. 7. Cyclic voltammogram for an electrolyte containing 0.025 M $CuSO_4$, 0.1 M $CoSO_4$, 0.7 M $NiSO_4$ and 0.265 M Na_3Cit. Rotation speed is 1200 rpm. Potentials sweep rate is 0.012 V s^{-1} and solution pH is 6.

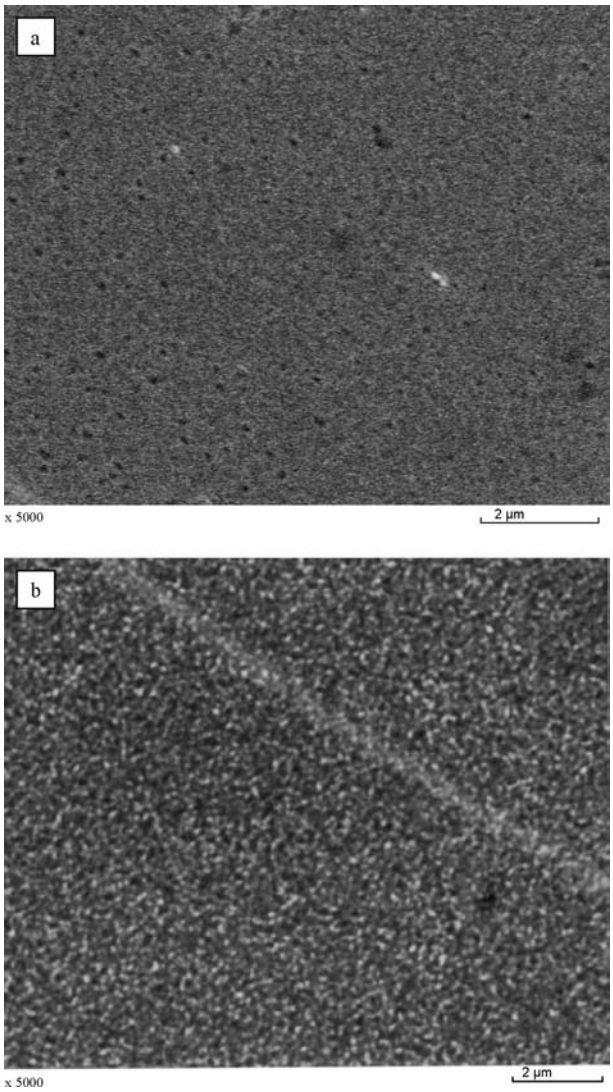

Fig. 8. Scanning electron micrographs of (a) Cu/Co–Cu/Cu and (b) Cu/Co–Ni–Cu/Cu sandwiches.

Co–Cu/Cu multilayers are less stable than Co–Ni–Cu/Cu ones plated from citrate electrolytes. Since a significant amount of Co–Cu can dissolve during the deposition of copper, the effect of this process should be considered during the fabrication of Co/Cu multilayers.

4. Conclusions

Cu/Co–Cu/Cu sandwiches have been deposited (by cyclic voltammetry) from 0.0125 M $CuSO_4$/0.25 M $CoSO_4$/0.26 M Na_3Cit electrolyte at pHs of 1.7 and 6.0. Calculations indicate that copper and cobalt are discharged from different species at the two different pHs. Two dissolution peaks were observed during the anodic dissolution of the deposit. Additional monitoring for metal ions at the ring showed that copper and cobalt dissolve independently from the sandwich at both pHs. Cobalt, the less noble metal, is dissolved first, followed by copper. Since, in each potential sweep, Cu/Co–Cu/Cu is formed, the cobalt is dissolved through a copper layer. It has been calculated that the copper overlayer is 600 nm, which suggests that the deposit is porous. SEM data indicated that Cu/Co–Cu/Cu sandwich deposit is porous whereas Cu/Co–Ni–Cu/Cu sandwich is not.

Acknowledgement

S.M.S.I. Dulal wishes to thank the Corrosion Research Centre at the University of Newcastle for a scholarship. The help from Dr T.A. Green for speciation calculations and a grant from DERA and Royal Society for the RRDE equipment and consumables are gratefully acknowledged.

References

1. S.K.J. Lenczowski, C. Schöenenberger, M.A.M. Gijs and M. Jonge, *J. Magn. Magn. Mater.* **148** (1995) 445.
2. G.R. Pattanaik, D.K. Pandya and S.C. Kashyap, *J. Electrochem. Soc.* **149** (2002) C363.
3. D.S. Lashmore and M.P. Dariel, *J. Electrochem. Soc.* **135** (1988) 1218.
4. S. Menezes and D.P. Anderson, *J. Electrochem. Soc.* **137** (1990) 440.
5. Y. Jyoko, S. Kashiwabara and Y. Hayashi, *J. Electrochem. Soc.* **144** (1997) L5.
6. A.R. Despić and V.D. Jović, *J. Electrochem. Soc.* **134** (1987) 3004.
7. D.M. Tench and J.T. White, *J. Electrochem. Soc.* **139** (1992) 443.
8. S. Roy, M. Matlosz and D. Landolt *J. Electrochem. Soc.* **141** (1994) 1509.
9. S. Roy and D. Landolt, *J. Electrochem. Soc.* **142** (1995) 3021.
10. P. Bradley, S. Roy and D. Landolt, *J. Chem. Soc., Faraday Trans.* **92** (1996) 4015.
11. P. Bradley and D. Landolt, *Electrochim. Acta* **42** (1997) 993.
12. P. Bradley and D. Landolt, *Electrochim. Acta* **45** (1999) 1077.
13. J.J. Kelly, P.E. Bradley and D. Landolt, *J. Electrochem. Soc.* **147** (2000) 2975.
14. J.J. Kelly, M. Cantoni and D. Landolt, *J. Electrochem. Soc.* **148** (2001) C620.
15. M. Shima, L. Salamanca-Riba and T.P. Moffat, *Electrochem. Solid State Lett.* **2** (1999) 271.
16. M. Alper, W. Schwarzacher and S.J. Lane, *J. Electrochem. Soc.* **144** (1997) 2346.
17. T.A. Green and S. Roy, 'Development of Stable Baths for the Electrodeposition of Multilayered Structures' Proceedings of the European Workshop on Electrodeposited CMA Coatings, (Athens, Greece, 28–29 May, 1997).
18. S. Nakamura and S. Mahajan, *J. Electrochem. Soc.* **127** (1980) 283.
19. W.J. Albery and M.L. Hitchman, 'Ring-Disc Electrodes', (Clarendon Press, Oxford, 1971).
20. W.J. Albery and S. Bruckenstein, *Trans. Faraday Soc.* **62** (1966) 1920.
21. MINEQL+. 'Chemical Equilibrium Management System', (Environmental Research Software, Hallowell, ME, 1994).
22. T.A. Green, A.E. Russell and S. Roy, *J. Electrochem. Soc.* **145** (1998) 875.
23. S.M.S.I. Dulal, E.A. Charles, L. Peter, I. Bakonyi and S. Roy, 'Giant Magnetoresistance in Electrodeposited Cu/Ni, Cu/Co and Cu/Ni–Co Multilayers' (Electrochem 2002, Preston, UK, 1–4th September, 2002).
24. S.M.S.I. Dulal, E.A. Charles and S. Roy, 'Composition Modulation in Ferromagnetic Layer in Ni–Co(Cu)/Cu Multilayer', (203rd Electrochemical Society Meeting, Paris, France, 27th April–02nd May, 2003).
25. W.R.A. Meuleman, S. Roy, L. Peter and I. Varga, *J. Electrochem. Soc.* **149** (2002) C479.